THE ANNALS OF "DUNAREA DE JOS" UNIVERSITY OF GALATI
FASCICLE XI – SHIPBUILDING. ISSN 1221-4620, e-ISSN 2668-3156
2021

NUMERICAL INVESTIGATIONS OF THE FREE SURFACE FLOW AROUND A SURFACE PIERCING HYDROFOIL

Costel Ungureanu
[1]University "Dunarea de Jos" of Galati,
Faculty of Naval Architecture, Galati, Domneasca
Street, No. 47, 800008, Romania,
E-mail:costel.ungureanu@ugal.ro
[2] Bureau Veritas Romania
165 Splaiul Unirii Street, TN Offices, 3rd Building,
B Wing, 5th Floor, 3rd District, 030133,
Bucharest, Romania,
E-mail:costel.ungureanu@bureauveritas.com

ABSTRACT

Starting with January 2013, naval architects face new challenges, as all ships greater than 400 tons must comply with energy efficiency index (MPEC 62, 2011). From ship hydrodynamics point of view, one handy solution is using Energy Saving Devices (ESD), with the main purpose to improve the flow parameters entering the propeller. For ballast loading condition the ESD may intersect the free surface disturbing and complicating the flow due to free surface /boundary layer interaction, turbulence and breaking wave effects that coexist and which are not completely clarified so far. Therefore, a free surface flow around a NACA 0012 surface piercing hydrofoil is numerically investigated and the results are compared to experimental results obtained in the Towing Tank of the Naval Architecture Faculty of "Dunarea de Jos" University of Galati. The comparison includes drag and free surface elevation on hydrofoil surface together with numerical uncertainty.

Keywords: free surface flow, NACA 0012, URANS, VOF, open channel flow

1. INTRODUCTION

Free surface flow is a hydrodynamic problem with a seemingly simple geometric configuration but with a complicated flow topology by the pressure gradient due to the presence of the obstacle, the interaction between the boundary layer and the free surface, turbulence, breaking waves, cavitation, water-air surface tension effects. As the appendages become more and more widely used and larger in size, the general understanding of the flow field around the appendages and the junction between them and the hull is a topical issue for naval hydrodynamics.

Due to the large difference in density between water and air, the flow around a profile that penetrates the free surface can be assimilated to the flow of a profile mounted on a plate. As long as the Froude numbers are small (Fn<0.1) and the deformation of the free surface is negligible, the flow topology is identical to that on a solid plate. The complexity of the junction at the level of the free surface increases with the Froude number, when the elevation of the surface becomes consistent, due to the freedom of movement on all three Cartesian directions of the water particles at the free surface.

The topology of the flow becomes much more complex when the phenomenon of

breaking the wave that interacts with the vortex horseshoe, also known as the vortex chain, is felt. Metcalf et al., (2006) investigates experimentally the interactions between the free surface and the boundary layer on a hydrodynamic profile, NACA 0024, at three Froude numbers (0.19, 0.37 and 0.55) associated with three different flow regimes : steady, with reattachment and without reattachment. At Fn=0.19, steady flow and Kelvin wave system are observed, while for Fn=0.37, the flow is manifested with the phenomenon of breaking the wave, but the streamlines are reattached on the hydrofoil surface while still maintaining the profile of Kelvin waves, while at Fn=0.55, the streamlines are no longer attached to body, the first wave ridge has a considerable height, the energy consumed when breaking the wave is high and the Kelvin wave system is no longer visible. Ungureanu (2011) tested a NACA 0012 hydrofoil in the Towing Tank of the Naval Architecture Faculty of "Dunarea de Jos" University of Galati, investigating the evolution of the free surface depending on the Froude number, $Fn \in \{0.32, 0.40, 0.48, 0.56, 0.64\}$. It was observed that, at relatively small Froude numbers, the wave on the surface of the profile has two ridges, and at large Froude numbers the bow wave is manifested with the phenomenon of wave breaking. Due to the increase in wavelength, the second wave ridge on the profile migrates to the flight edge, leaving the profile at high speeds. At high speed, the wave generated by the trailing edge becomes prominent, taking the form of a whale tail, with a height close to that of the leading edge.

In this study, the free surface flow around a NACA 0012 surface piercing hydrofoil is numerically investigated and the results are compared to experimental results obtained by Ungureanu (2011).

2. NUMERICAL MODEL

2.1. Boundary Conditions

The numerical hydrofoil has the same dimensions as the experimental model, namely 0.5 m chord and 1.2 m wingspan (figure 1) .

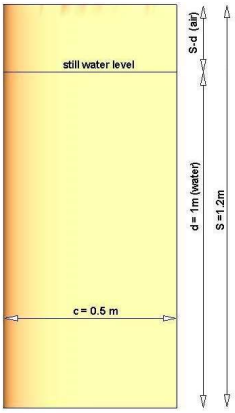

Fig.1. Hydrofoil dimensions

When flowing with a free surface, the surface piercing hydrofoil generates a divergent waves system propagating at an angle of approximately 20°. In order to avoid the radiation of the waves upstream, the inlet boundary is positioned at 1 span length upstream of the profile. In order to avoid the reflection of the wave system from the lateral boundaries, producing numerical instabilities, the width of the calculation domain, as well as the length of the downstream area are established so that the wave system leaves the integral domain through the downstream boundary. Therefore, the downstream boundary is arranged at two span lengths from the profile trailing edge, and the side boundaries at two span lengths from the hydrofoil plane of symmetry. The position of the upper boundary is chosen so as to allow the natural elevation of the free surface (figure 2). Also, the computational domain extends one span below the profile and half a span above the profile thus avoiding the influence of possible end vortices and limited bottom effect.

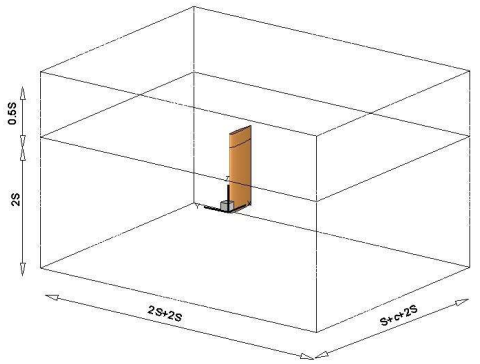

Fig.2. Computational model (S- span, c- chord)

The boundary conditions, shown in figure 3, have been chosen to be compatible with the "open channel flow" calculation option in Fluent, namely pressure boundaries with the imposition of the velocity and level of the calm free surface on the inlet and outlet boundaries. The wall condition was imposed on the profile, and the sliding wall was imposed on the other boundaries.

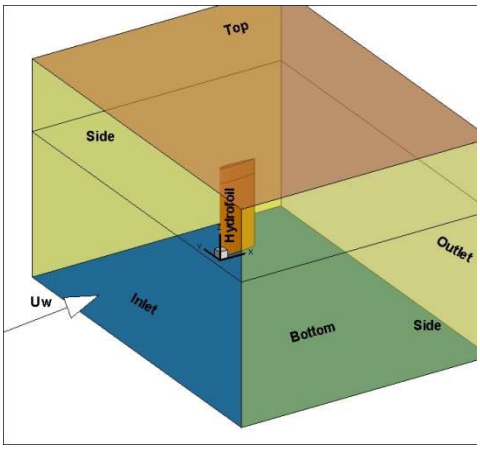

Fig.3. Boundary conditions

2.2. Numerical schemes

Using Ansys 12.1 program, the URANS equations were solved in a segregated manner, supplemented by the equations of the turbulence model suitable for free surface calculations. In this case, two turbulence models with two equations were tested, k-ω SST and k-ε Realizable. For the calculation of the free surface, the VOF technique was used, considering the free surface as an iso-surface of 0.5 water / air. The coupling of pressure and velocity was solved with the PISO algorithm. The pressure was discretized with the PRESTO numerical scheme, for the free surface the geometric reconstruction was used, and for the convective and difussive terms the QUICK scheme was used.

In the present study, the explicit, quasi-stationary calculation with advancement in time, proved to be a much more robust and stable alternative than the stationary calculation. Fluent's calculation algorithm is quite robust and allows advancement over time without distorting the results. In order not to introduce errors in the calculation, when integrating the flows on the cells, the time step necessary to integrate the flow equations is calculated based on the volume of the smallest cell in the discretization network. The solution of the URANS equations system was obtained in about 4000 time steps, after the convergence of the drag and the free surface, with the convergence obtained in a maximum of 20 iterations per time step. The calculations were performed for all 12 experimental velocities and for all 4 drafts.

2.3. . Grid Generation

The discretization grid is C-H with normal grid lines on the hydrofoil surface respecting the distance to the dimensionless and rectangular wall in the vertical direction. In the the free surface elevation area the grid lines are denser and equidistant, having 1.5 mm height relaxing towards the end of the profile, as it can be seen in figure 4.

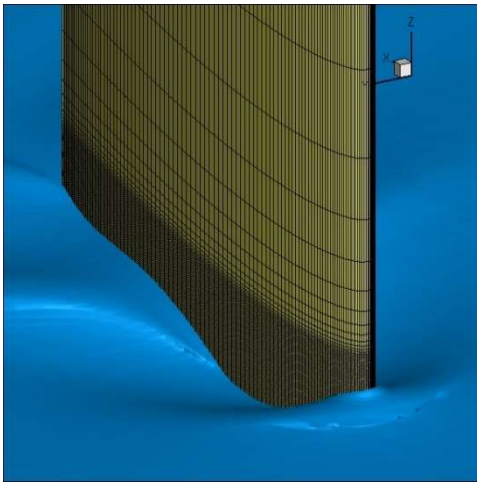

Fig.4. Gridlines on the hydrofoil surface

3. RESULTS AND DISCUSSIONS

3.1. . Numerical Uncertainty

For the numerical calculations required for validation, three sources of possible errors were identified: truncation errors, iterative errors and discretization errors. The double precision solver was used and in this way the truncation errors were neglected. The iterative errors were neglected, decreasing the implicit residue value from 10^{-3} to 10^{-4}, obtaining at the same time the convergence on each time step. As a result, the analysis of errors and uncertainties focused on discretization errors, the ones with the largest value in the numerical calculation.

Three discretization grids (Table 1) were generated with $\sqrt{2}$ as refining ratio, according to ASME V&V 20 (2009). The $y^+ = 1$ as the nondimensioned wall distance was used for all grids, so that the boundary layer to be calculated in the same manner by the turbulence models.

Table 1. Generated grids

Grid	Fine (1)	Medium (2)	Coarse (3)
N_i	2425174	1212587	606294
$\sum V_i$ [m^3]	59.04	59.04	59.04
h_i [m^3]	0.00493	0.00698	0.00987
r21		1,414	
r32			1,414

Hydrofoil drag is considered as a reference value, and based on the 3 grids the discretization uncertainty or the convergence index of the grid is calculated, as it is also known in the literature. Below, there are tabulated the values of the drag for all three grids studied together with the discretization error and the uncertainty of the error.

Table 2. K-ω SST drag errors and uncertainties

Fn	Fine	Medium	Coarse	δG[%]	IG[%]
	Drag [N]				
0.16	0.92	0.95	0.97	3.62	4.52
0.24	1.77	1.85	1.88	3.58	4.48
0.32	3.47	3.65	3.72	3.42	4.27
0.40	5.81	6.13	6.26	3.65	4.56
0.48	8.95	9.85	10.21	6.67	8.33
0.56	13.60	15.10	15.70	7.21	9.01
0.64	17.37	19.35	20.24	9.36	11.70
0.72	20.05	22.47	23.81	14.76	18.46
0.80	22.74	26.45	28.61	22.77	28.47
0.88	25.21	29.83	32.42	23.56	29.45
0.96	27.89	33.86	36.88	21.80	27.25
1.04	30.80	38.66	42.51	24.52	30.65

Table 3. K-ε Realizable drag errors and uncertainties

Fn	Fine	Medium	Coarse	δG[%]	IG[%]
	Drag [N]				
0.16	1.21	1.25	1.27	2.52	7.57
0.24	2.63	2.74	2.80	6.18	7.72
0.32	4.43	4.66	4.78	6.72	8.40

0.40	6.76	7.16	7.37	7.04	8.80
0.48	10.97	12.30	12.78	6.91	8.64
0.56	15.36	17.12	17.80	7.13	8.91
0.64	19.86	22.33	23.62	13.66	17.08
0.72	23.17	26.04	27.75	18.35	22.94
0.80	26.26	30.60	33.22	25.38	31.73
0.88	29.14	35.34	38.92	29.11	36.39
0.96	32.69	39.98	44.00	27.43	34.29
1.04	36.26	45.87	50.84	28.36	35.45

It is observed that in the area of large froude numbers, where the phenomenon of breaking the wave is consistent, the level of uncertainties is higher than in the area of froude numbers where the free surface is not affected by the broken wave. The basic principle of VOF theory says that the two fluids considered in the calculation are immiscible, and how the phenomenon of breaking the wave manifests itself with a mixture of air bubbles in water, and this can lead to a high degree of uncertainty. Another possible source of errors and uncertainties at high speeds is the grid itself. As the wave elevation grew, the grid area for the free surface had to be increased so as to cover the entire elevation of the wave on the body. For reasons of hardware resources, the calculation went on a single fine grid for all speeds, hence and probably the high level of uncertainty at high speeds.

3.2. .Numerical/ experiment comparison

The numerical drag (CFD) was calculated for both turbulence models tested and compared with the experimental results (EFD), and shown for the 1m draft in figure 5. It is observed that qualitatively both turbulence models describe the evolution of the drag in relation to the Froude number, but quantitatively the k-ω SST turbulence model produces results by 60%, on average, compared to the experimental ones compared to 85% obtained with the k-ε Realizable model.

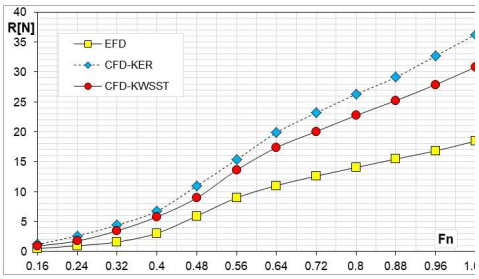

Fig.5. Drag comparsion CFD vs EFD, 1m draft

Next tables are presenting the experimental and numerical results obtained with the fine grid, together with the comparison error, E, the numerical uncertainty, D, as well as the validation uncertainty, I_{val}. It is pointed out that the comparison error is lower than the validation uncertainty, as a result the modeling errors are insignificant.

Table 4. K-ω SST numerical uncertainty

Fn	Drag [N]		E [%]	Usn [%]	Ue [%]
	EFD	**CFD-K-ω SST**			
0.16	0.506	0.925	82.77	4.52	82.9
0.24	0.982	1.775	80.75	4.48	80.9
0.32	1.597	3.475	117.59	4.27	117.7
0.4	3.062	5.805	89.59	4.56	89.7
0.48	5.936	8.953	50.82	8.33	51.5
0.56	8.972	13.595	51.53	9.01	52.3
0.64	11.019	17.368	57.62	11.70	58.8
0.72	12.607	20.047	59.01	18.46	61.8
0.80	14.047	22.739	61.88	28.47	68.1
0.88	15.463	25.214	63.06	29.45	69.6
0.96	16.829	27.895	65.75	27.25	71.2
1.04	18.458	30.804	66.89	30.65	73.6

Table 5. K-ε Realizable numerical uncertainty

Fn	Drag [N]		E [%]	Usn [%]	Ue [%]
	EFD	**CFD-K-ω SST**			
0.16	0.506	1.211	139.27	7.57	139.5
0.24	0.982	2.628	167.66	7.72	97.1

0.32	1.597	4.430	177.38	8.40	96.6
0.4	3.062	6.757	120.69	8.80	92.9
0.48	5.936	10.969	84.79	8.64	79.2
0.56	8.972	15.356	71.16	8.91	71.2
0.64	11.019	19.862	80.25	17.08	68.4
0.72	12.607	23.166	83.75	22.94	66.6
0.80	14.047	26.264	86.97	31.73	69.1
0.88	15.463	29.135	88.42	36.39	68.6
0.96	16.829	32.691	94.25	34.29	64.0
1.04	18.458	36.262	96.46	35.45	61.9

The numerically calculated waves are compared with the experimental waves and presented graphically in figure 6, for the Froude numbers 0.32, 0.48 and 0.64. The abscissa of the diagrams represents the level of calm free-surface, and the values presented were dimensioned with the length of the foil chord.

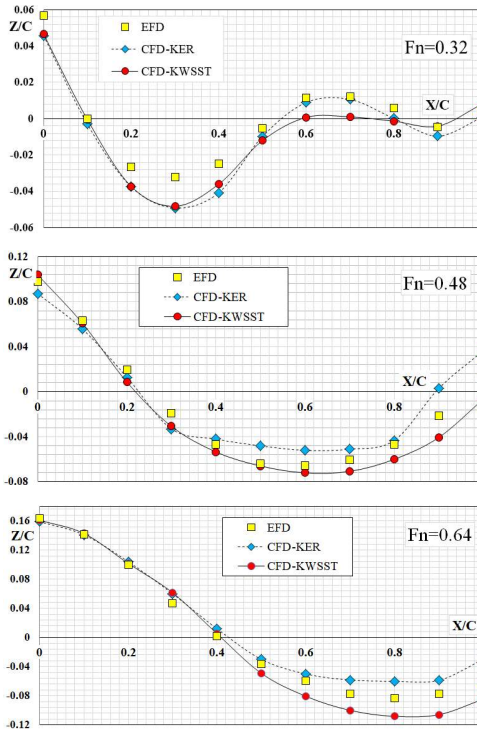

Fig.6. Wave profile comparsion

Qualitatively, both turbulence models capture the elevation of the free surface on the hydrofoil surface. Quantitatively, it is observed that, in the area of leading edge, both models of turbulence manage to capture the development of the experimental wave at close values. The k-ω SST model underestimates the wave gap, which is visible in all three Froude numbers, but also the second wave ridge at Fn = 0.32, while the k-ε Realizable model overestimates the wave gap, and at Fn = 0.32, it manages to approach of the second wave ridge.

Figure 7, 8 and 9 comparatively show the topology of the free surface observed experimentally (left) and numerically (center), and on the right, the free surface as a colored isosurface in elevation contours. The calm water line is drawn on the numerical hydrofoil, similar to the one drawn on the experimental model. The flow at Fn = 0.32, shows the development of the Kelvin wave system. As the Froude number increases, the wavelength increases and the influence of the blocking edge of the attack board on the flow around the profile increases.

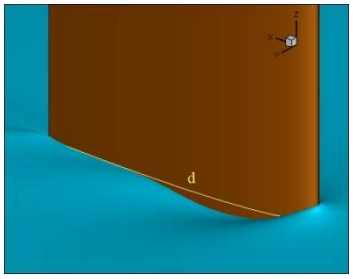

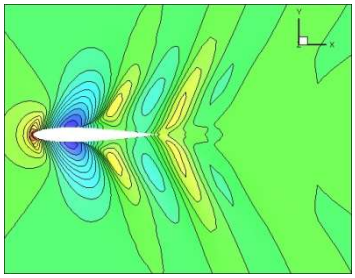

Fig.7. Free-surface comparison, Fn =0.32

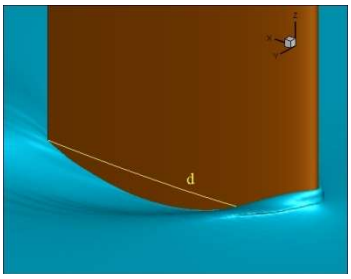

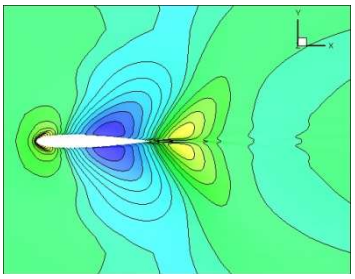

Fig.8. Free-surface comparison, Fn =0.48

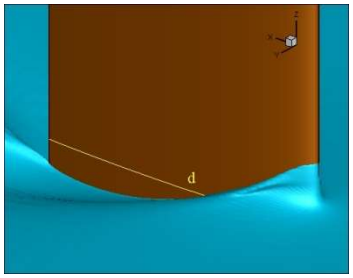

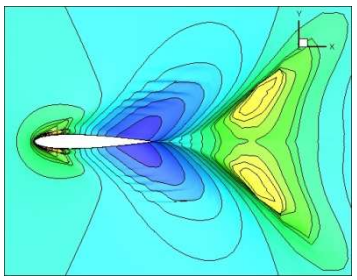

Fig.9. Free-surface comparison, Fn =0.64

4. CONCLUDING REMARKS

A numerical study on the free-surface flow around a NACA 0012 surface piercing hydrofoil was presented. Two turbulence models implemented in Ansys Fluent were tested and the results were compared with the experimental ones. By Froude similarity, the height of the wave in the area of the leading edge can be approximated so that the discretization grid accurately captures the deformed free surface.

Acknowledgements

This research study was performed in the frame of Multidisciplinary Research Platform ReForm "Dunarea de Jos" University of Galati - The Naval Architecture Research Center.

REFERENCES

[1]. International Maritime Organization, MEPC 62nd session, 11-15 July, 2011;

[2]. **Ungureanu, C., „***Experimental Uncertainty for the Galati University Towing Tank Tests with Example for NACA 0012 Surface Piercing Hydrofoil"*, Annals of "Dunarea de Jos" University Galati. Fascicle XI, Shipbuilding, pp. 133-140, 2012;

[3]. **Ungureanu, C.,** *„Towing Tank Experiments for a Surface Piercing NACA 0012 Hydrofoil"*, Annals of "Dunarea de Jos" University Galati. Fascicle XI, Shipbuilding, pp. 5-10, 2011;

[4]. ASME V&V 20, *Standard for Verification and Validation in Computational Fluid Dynamics and Heat Transfer*, 2009;

[5]. **Roache, P. J,** *"Quantification of uncertainty in computational fluid dynamics",* Annu. Rev. Fluid. Mech., 29:123–60, 1997;

[6]. **Metcalf B., Longo J., Ghosh S., Stern F.,** *"Unsteady free-surface wave-induced boundary-layer separation for a surface-piercing NACA 0024 foil: Towing tank experiments",* Journal of Fluids and Structures 22 (2006) 77–98;

Paper received on November 16th, 2021

